JME

Journal of Mining & Environment,
Vol.9, No.2, 2018, 339-348.
DOI: 10.22044/jme.2017.6156.1430

Technical Note

Effect of thermal treatment on specific rate of breakage of manganese ore

M. Heshami and R. Ahmadi*

Department of Mining Engineering, College of Engineering, Imam Khomeini International University, Qazvin, Iran

Received 22 August 2017; received in revised form 25 October 2017; accepted 26 October 2017
Corresponding author: ra.ahmadi@eng.ikiu.ac.ir (R. Ahmadi).

Abstract
The aim of this work is to investigate the effect of thermal treatment on the grinding behavior of manganese ore in the various size fractions of -1.7+1.18, -1.18+0.6, -0.6+0.3 and -0.3+ 0.15 mm. Breakage Function Determination Software (BFDS) is used to calculate the selection function of the experiment. The results of SEM analysis show the micro-cracks in the thermally treated manganese sample, and DTA/TG analysis show that heating at 750 °C leads to dehydroxylation of montmorillonite, and decomposition of calcite and decomposition of montmorillonite to silicate minerals occur at 850 °C. Montmorillonite mineral with a hardness of 2 is turned into silicate minerals with an average hardness of 7. Therefore, it can be seen that the thermal treatment leads to a decrease in the specific rate of breakage from 1.04 min^{-1} to 0.65 min^{-1} (approximately to 37%) for a size fraction of -0.300+ 0.15 mm. It; can be expressed that the thermally treated sample is broken more slowly than the untreated sample. Also, parameter "A" is the maximum S_i value, decreasing for the heated sample from 4.36 min^{-1} to 4.28 min^{-1}. The selection function results show that all size fractions of this material follow a first-order kinetics.

Keywords: *Thermal Treatment, Specific Rate of Breakage, Grinding Kinetics, Breakage Function Determination Software, Manganese Ore.*

1. Introduction

The comminution process is extensively applied in industries such as mineral processing, ceramics, and chemical industries [1]. Two mineral processing problems, energy consumption and mineral recovery, have dominated research works in comminution. Comminution in the mineral processing industry includes two processes, crushing and grinding. It has been estimated that comminution processing is the most energy consuming stage in mineral processing and grinding is a more energy consuming process than crushing [2]. Therefore, in order to make the grinding more efficient, details should be considered carefully [3-4]. The breakage kinetics in the mills has been developed as a practical model. Selection function conception is used to analyze grinding in the ball mill [5]. Therefore, the selection function is a main parameter for:

- Ball and rod mill circuits simulation
- Simulating the grinding mechanisms in mill and determining the dominant mechanisms
- Simulating the material movement in mill
- Investigating the mill performance and improving the operating parameters, while there are mechanical defects in grinding [6-7].

It is known that developing the pretreatment methods could significantly decrease the energy consumption. Conventional heating is one of the Thermal treatment methods in which heat is transferred from the outside inward through standard heating mechanisms [8]. Microwave heating is fundamentally different from conventional heating, as opposed to conventional thermal processing because microwave is a non-ionizing electromagnetic radiation and can penetrate deep into the sample.

One of the major applications of thermal treatment is assisting grinding processing. Vorster

et al. (2001) have studied the influence of microwave radiation on the grindability of copper-zinc ores. The results obtained showed that 50% reduction in the strength of ore happened after 90s of microwave radiation [9]. Sikong and Bunsin (2009) have carried out an investigation on the thermal treatment of granite rock. The results obtained showed that the strength of treated granite was less than 60% of the original after 30 minutes of exposure [10]. Also Zhao et al. (2014) have studied the effect of microwave treatment on the selective heating behavior, and the magnetic separation characteristics of ilmenite ore have been investigated. The results obtained showed that micro-cracks appeared at grain boundaries of ilmenite ore after microwave treatment. Also the results of magnetic separation showed that magnetic separation characteristics of the treated samples were better than the untreated ilmenite samples [11]. Few studies have focused on the effect of thermal treatment on grinding kinetics, out of which the following can be mentioned. Kumar et al. (2010) have investigated the effect of microwave treatment on the specific rate of breakage of iron ore. The results obtained showed that microwave pretreatment led to an increase in the specific rate of breakage value for a fraction size of -19.5+12.7 mm up 50% [12]. Also Koleini et al. (2012) have investigated the effect of microwave treatment on the grinding kinetics of iron ore. The results obtained showed that the specific rate of breakage (Si) increased by an average of 50%. In addition, it was found that microwave-treated iron ore produced a coarser material than untreated iron ore by considering the γ value of $B_{i,j}$ [13].

In this work, the effect of thermal treatment by muffle furnace on the grinding behavior of manganese ore was investigated by the specific rate of breakage (S_i). The thermal mechanism is fundamentally different from microwave heating, and previous studies have been carried out on microwave, so this work has been done for the first time. Phase transformations and structural changes in the sample were explained by thermal analysis (DTA/TG), and scanning electron microscope (SEM) images.

2. Modeling

The selection function or specific rate of breakage is a measure of grinding process kinetics. In other words, it is an indication of how fast the material breaks. The selection function is defined as the fraction by weight of particles of given size i that are selected and broken per unit times of grinding. The value varies with size [6].

There is a sample experimental evidence that batch grinding of brittle and homogeneous materials follows a first order kinetics (Eq.2) [1, 14, 15].

$$\frac{dw_i(t)}{dt} = -S_i w_i(t) \quad (1)$$

$$w_i(t) = w_i(0) e^{-S_i(t)} \quad (2)$$

When Eq. (2) is integrated, Eq. (3) is obtained:

$$\ln\left(\frac{w_i(t)}{w_i(0)}\right) = S_i t \quad (3)$$

where, S_i is a proportionality constant called the specific rate of breakage of feed size material with the unit of time^{-1}, $W_i(t)$ and $W_i(0)$ are the mass fractions of the top size fraction at times (t) and 0, respectively.

The equation proposed for variation in the specific rate of breakage (S_i) with particle size is [16-18]:

$$S_i = A\left(\frac{X_i}{X_0}\right)^{\alpha} Q_i \quad (4)$$

In this equation, X_i is the maximum size of the screen interval indexed i (mm), X_0 is the standard size that it is considered 1 mm here, and A and α are the model parameters depending on the material and the milling condition. Q_i is a correction factor which is 1 for smaller sizes (normal breakage) and less than 1 (abnormal breakage) for particles that are too large to be nipped and fractured properly by the ball size in the mill. In an abnormal breakage region, values for Q_i are empirically described by:

$$Q_i = \frac{1}{1 + \left(\frac{x_i}{\mu}\right)\lambda} \quad (5)$$

where μ is the particle size when the correction factor is 0.5, and λ is a positive number (λ> 0) and an index of how rapidly the rates of breakage fall as size increases that are the higher than the value of λ, the more rapidly the values decrease [7, 13, 16].

3. Materials and methods

3.1. Mineralogy and identify of the manganese ore

The sample used in this work was obtained from Venarj Manganese Mining located in Qom, Iran. For identification of the types of minerals in the

sample, an X-ray diffraction (XRD) analyzer (model PW1800) with a copper tube was used. The XRD analysis showed that the main minerals of the sample included hematite (Fe_2O_3), braunite ($Mn^{2+}Mn_6^{3+}SiO_{12}$), quartz (SiO_2), and calcite ($CaCO_3$), and the minor minerals were montmorillonite clay mineral ($(Ca_{0.2}(Al,Mg)_2Si_4O_{10}(OH)_2,XH_2O)$, orthoclase ($KAlSiO_3O_8$), and albite ($Na,Ca(Si,Al)_4O_8$) (Figure1).

SEM and energy dispersive X- ray spectroscopy (EDS) analyses were carried out to identify the minerals present in the sample, and the results obtained were shown in Figure 2. The results obtained indicated that braunite was the major manganese mineral in the sample (bright gray) (Figure 2A, EDS 1). Quartz mainly disseminated in rock matrix, as shown in (Figure 2A, EDS 2). Orthoclase and albite minerals were present at the edge surrounding the braunite grains (Figure 2A, EDS 3 and EDS 4). Braunite was inter-locked with quartz, orthoclase and albite of mainly triple types (Figure 2A), which decreased with particle size.

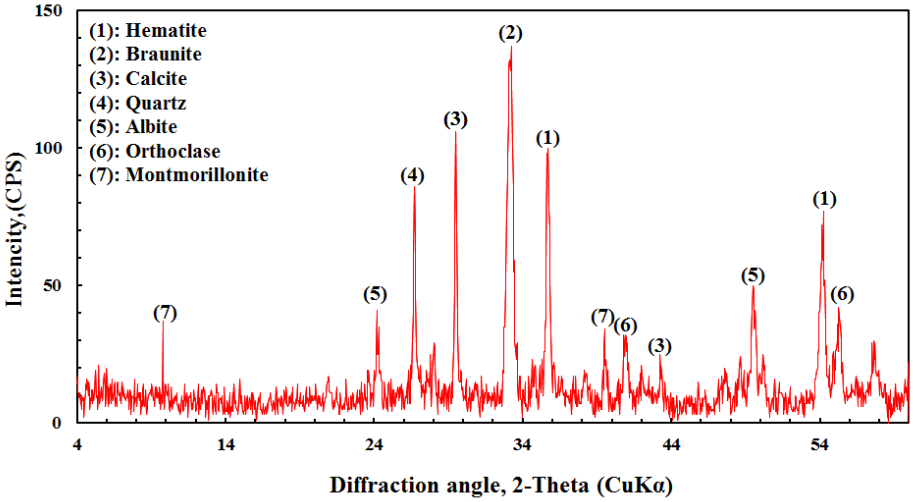

Figure 1. XRD pattern for manganese ore.

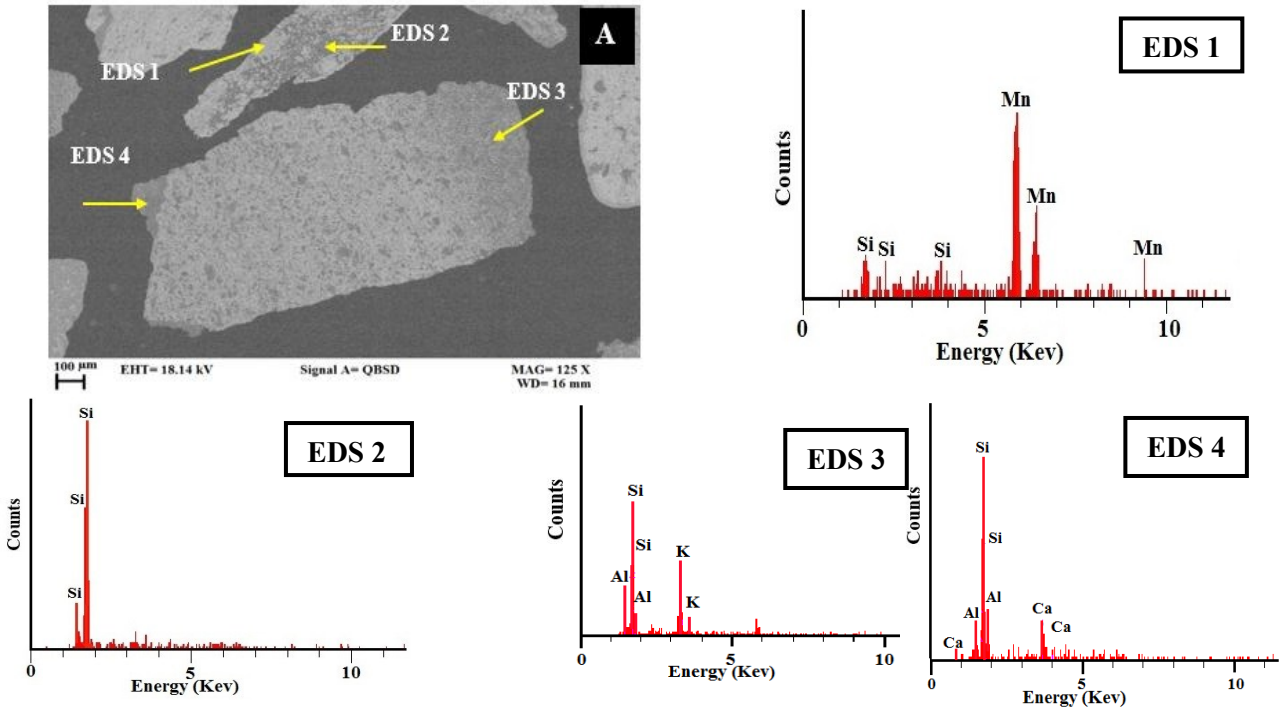

Figure2. SEM image (A) of manganese ore; energy dispersive X- ray spectroscopy of points (EDS 1, EDS 2, EDS 3, and EDS 4).

3.2. Phase and structure changes during thermal treatment

In order to study the phase transformations of the sample in different temperatures, thermal analysis using DTA/TG (model STA409PC LUXX, NETZSCH, Germany) was carried out. For this purpose, 46 mg of the ore sample was used for the analysis, and also alumina was used as the reference substance. The thermal analysis of the sample was done from 22 ℃ to 1000 °C with a heating rate of 10 °C/min in the atmospheric condition. In addition, for observation, cracks were created in samples due to thermal treatment using a scanning electron microscope SEM (model LEO1430VP, Germany and England). To evaluate the effect of thermal treatment, one sample was treated in a muffle furnace (model AWF 12/25, Lenton, England) and was compared with the untreated sample.

3.3. Grinding test

In order to investigate the influence of thermal treatment on grinding kinetics, the selection function or specific rate of breakage (S_i) was used. Single-size fractions of feed, i.e. -1.7+1.18, -1.18+0.6, -0.6+0.3, and -0.3+0.15 mm, were prepared. Two samples from each fraction weighting 300 g were prepared. One sample was thermally treated for 60 min in 750 °C, and was compared with the untreated sample. Grinding tests were performed in a laboratory ball mill with a 20 cm diameter, a 25 cm length, and the critical speed of 76 rpm (80% of the critical speed). The mill charge consisted of stainless steel balls with diameters ranging 15–40 mm, and the total weight of the grinding charge was 8.869 kg. The BFDS (Breakage Function Determination Software) was used for calculation of the selection function of the experiment; this software is able to calculate the breakage and selection function parameters [19].

4. Results and discussion

4.1. Phase and structure changes during thermal treatment

4.1.1. Thermal analysis (DTA/TG)

The DTA-TG curves for the sample are shown in Figure 3. Based on the Differential Thermal Analysis (DTA) curve, the first endothermic peak at 100 °C is associated with evaporation of moisture or physically bound water (Eq. 6), which corresponds to a weight loss of ca. 1%. The weight loss continued until the temperature reached 600 °C, which is due to the dehydroxylation of montmorillonite clay mineral (exiting the hydroxyl ions from the montmorillonite structure) in the sample (Eq. 7). This alteration continued until the temperature reached 775 °C. The weight loss of ca. 5% observed at 600-775˚C can be attributed to the dehydroxylation of montmorillonite and calcite decomposition in this temperature range (Eq. 9) [20-24]. The second endothermic peak in 750 °C happened because of the same reason. The exothermic peak at 850 °C and the weight loss from 775 to 1000 °C are due to the decomposition of montmorillonite to silicate minerals (cristobalite, mullite, spinel, and cordierite) (Eq. 8) [22, 23].

$$Ca_{0.2}(Al,Mg)_2Si_4o_{10}(OH)_2,H_2O \rightarrow Ca_{0.2}(Al,Mg)_2Si_4O_{10}(OH)_2 + XH_2O \quad (6)$$

$$Ca_{0.2}(Al,Mg)_2Si_4o_{10}(OH)_2 + O_2 \rightarrow Ca_{0.2}(Al_2O_3.2SiO_2.2MgO.SiO_2) + H_2O \quad (7)$$

$$\begin{aligned} &Ca_{0.2}(7Al_2O_3.4Sio_2.4MgO.4SiO_2)_2 \rightarrow \\ &3Al_2O_3.2SiO_2 + 2(MgO.Al_2O_3) + SiO_2 + 2MgO.2Al_2O_3.5SiO_2 + Ca\downarrow \end{aligned} \quad (8)$$

$$CaCO_3 \rightarrow CaO + CO_2 \quad (9)$$

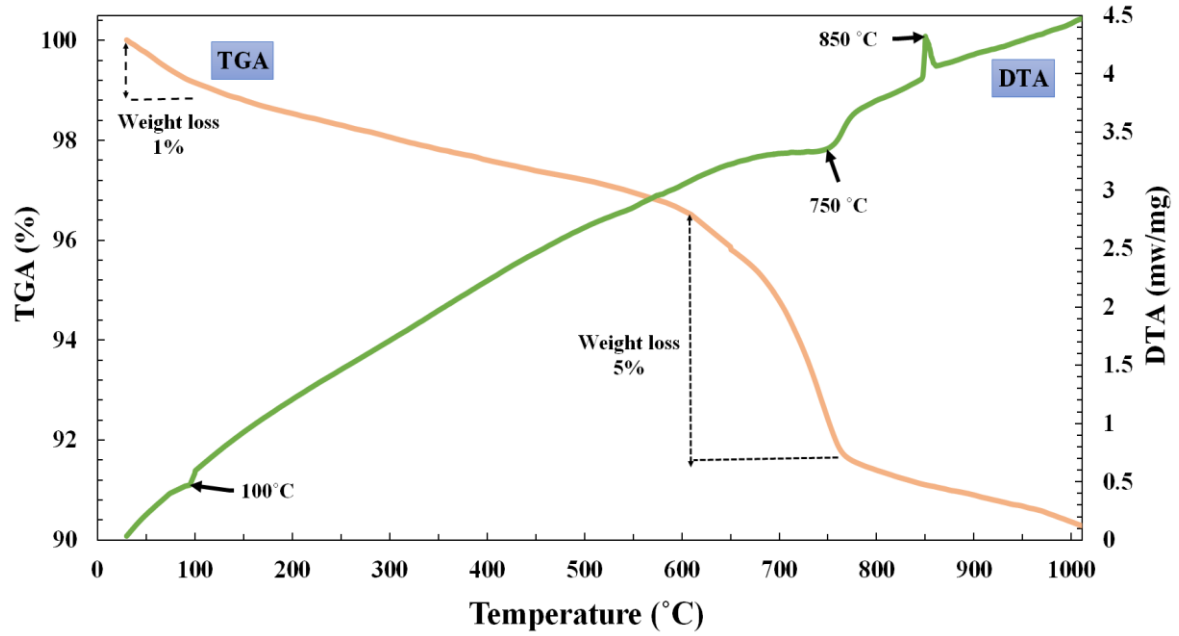

Figure3. Thermal analysis (DTA/TG) of manganese ore (experimental conditions: sample weight, 46 mg; heating rate, 10 ˚C/min; reactive gas, air; reference substance, Al_2O_3).

4.1.2. SEM analysis

Figure 4 shows the scanning electron micrograph of the thermally treated and untreated samples. The SEM micrograph shows the thermal treatment induced micro-fractures in the ore. The main reason for facture induction is the α-β quartz inversion at 573 ˚C, leading to a crystal volume increase of 2% [25]. This along with anisotropic expansion of quartz crystals causes the inter-granular structure to build up throughout the structure (cracks and fractures). Other reason for sample cracking during thermal treatment are calcite decomposition and CO_2 gas emission (Eq.9).

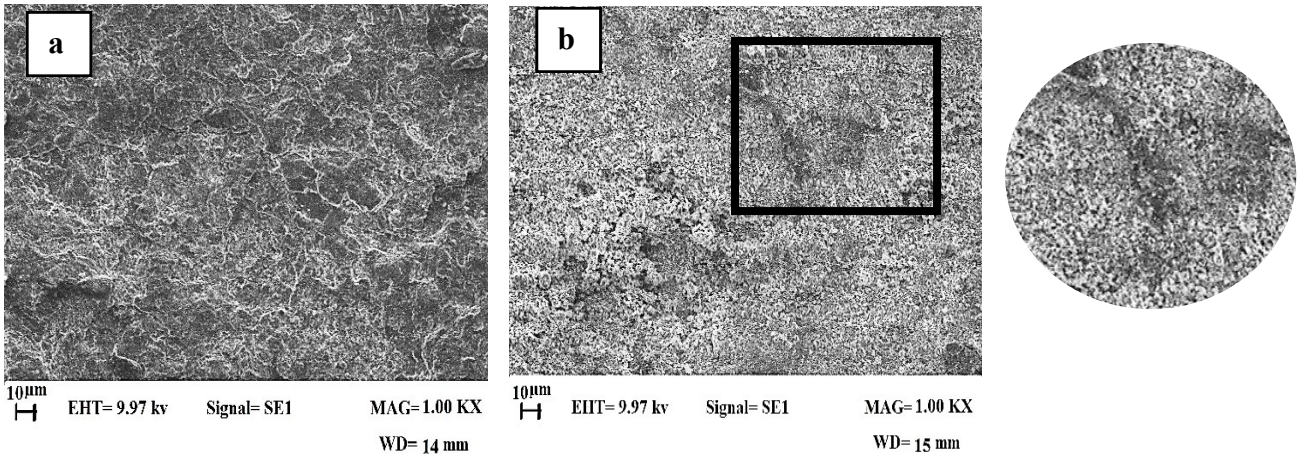

Figure4. Scanning electron micrograph of untreated manganese ore; (b) scanning electron micrograph of manganese ore treated at 750 ˚C for 60 minutes.

4.2. Effect of thermal treatment on specific rate of breakage (S_i)

4.2.1. Effect of mass retained

The selection function was calculated using the BFDS software. In order to determine the specific rate of breakage for size fractions, semi-logarithmic curves of the mass remained on the screen *vs*. the grinding time were plotted for untreated and thermal treated samples in Figures 5 and 6, respectively. As it can be seen in these figures, the breakage process follows a first-order behavior for all size fractions.

The specific rates of the breakage values were estimated using the average slopes of the plots, and the equations related to the lines in various size fractions are given in Figures 5 and 6. The Si values for various size fractions in both the untreated and thermal treated samples are shown in Tables 1 and 2, respectively. The results obtained show that the specific rate of breakage for size fraction of -0.300+0.15 mm decrease after thermal treatment (approximately to 37%). Based upon the DTA/TG results, heat caused the decomposition of clay minerals and transformation to silicate minerals (cristobalite, mullite, spinel and cordierite) having higher hardness (Table. 3). Montmorillonite mineral with a hardness of 2 was turned to silicate minerals with an average hardness of 7. The clay mineral changes (increasing resistant of clay mineral) (Table. 1) overcome the micro-cracks occurred, which was caused by phase transformations of quartz and calcite decomposition. Thus with particle size reduction, structural changes in the sample affect the comminution behavior.

Previous research works carried out by Kumar et al. (2010) and Koleini et al. (2012) showed that after microwave treatment, the specific rate of breakage (Si) increased by an average of 50%. This implies that the sample under microwave treatment is broken faster than the untreated sample [12, 13]. Therefore, in this work, the specific rate of breakage values for the thermally treated sample in comparison with the untreated sample decreased. It can be expressed that the thermally treated sample is broken slower than the untreated sample.

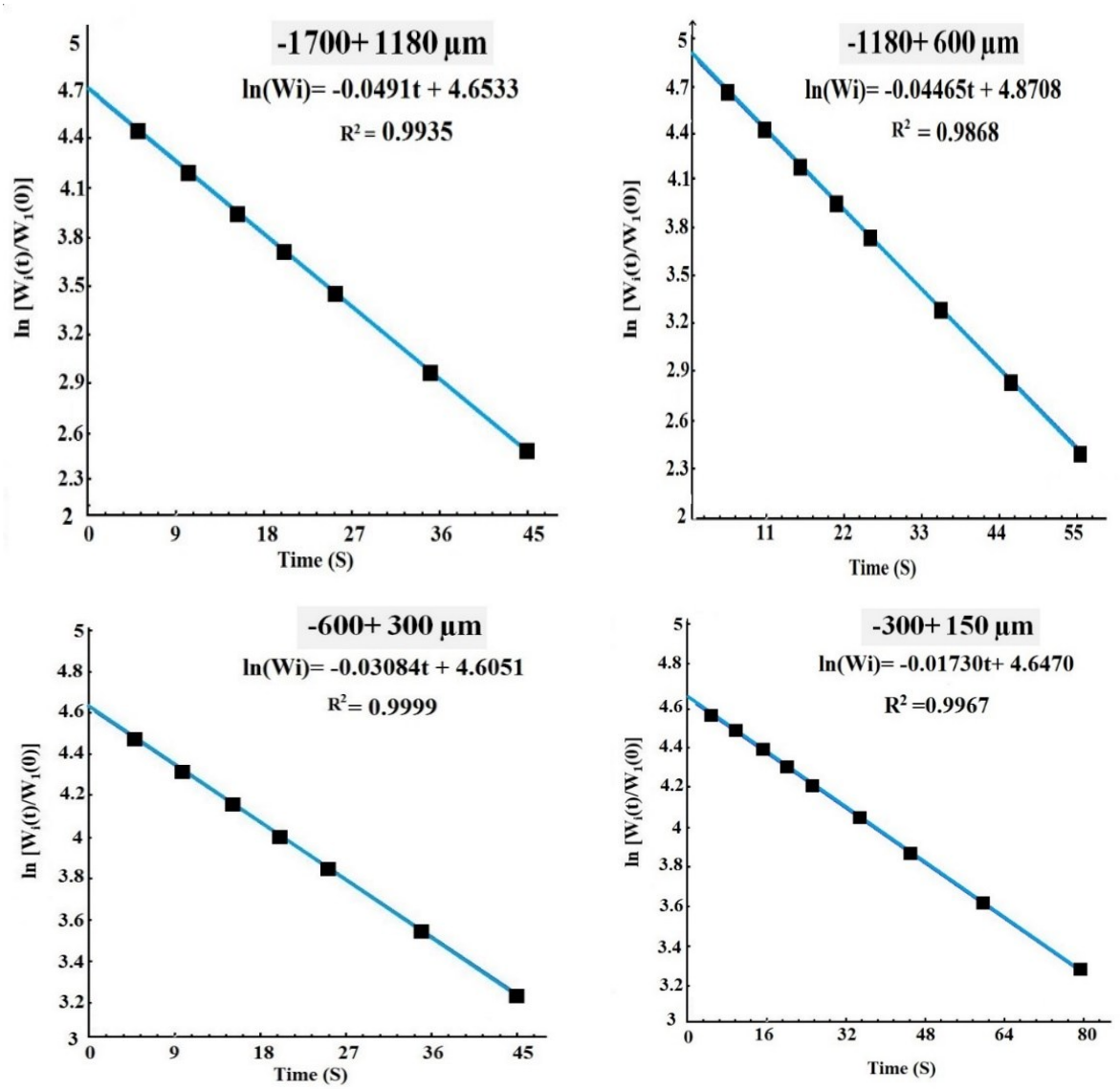

Figure5. First-order plots of various size fractions for untreated sample.

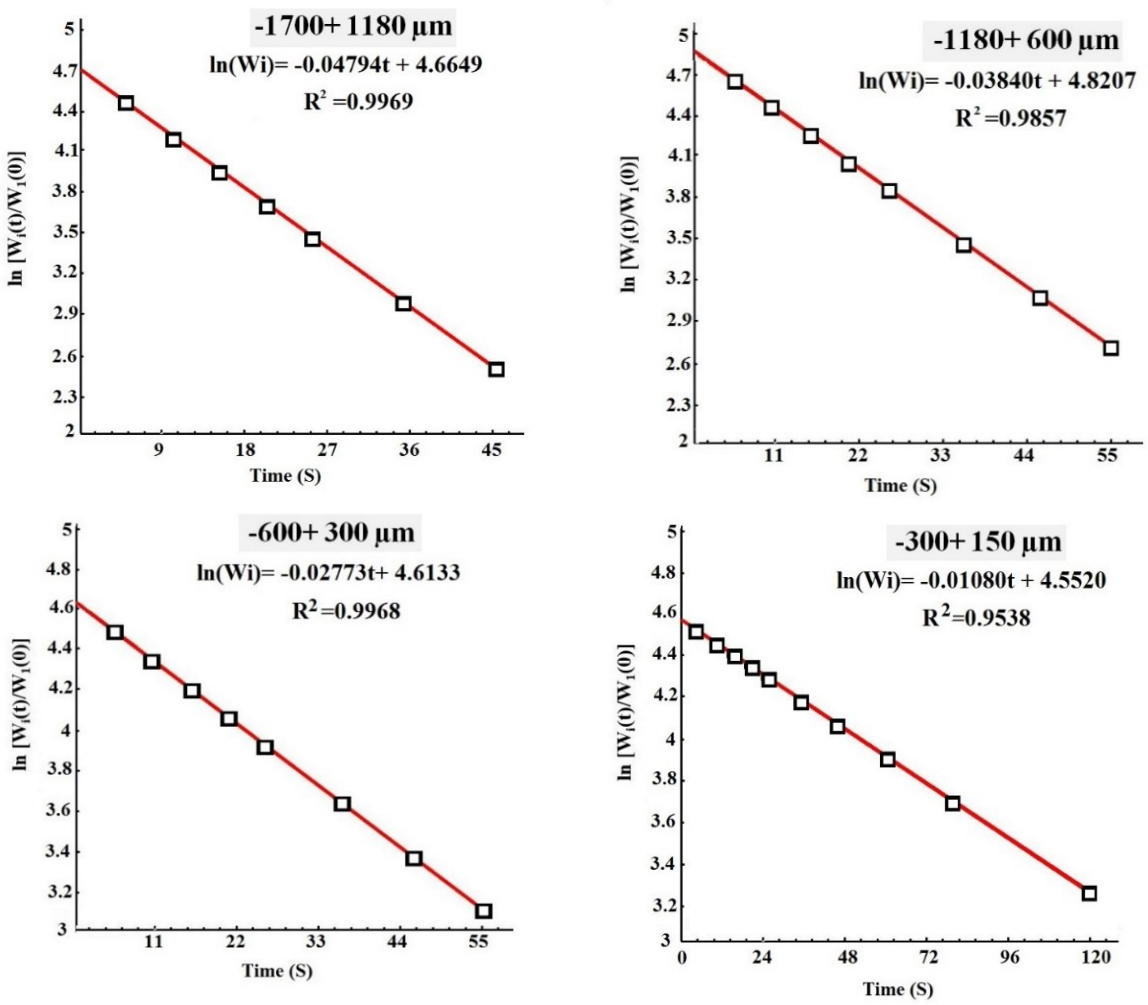

Figure 6. First-order plots of various size fractions for thermally treated sample.

Table 1. Specific rates of breakage for various size fractions for untreated samples.

Size fractions (mm)	Specific rate of breakage	
	S^{-1}	$min^{-\oplus}$
-1.7+ 1.18	0.0491	2.95
-1.18+ 0.6	0.04465	2.68
-0.6+ 03	0.03084	1.85
-0.3+ 0.15	0.0173	1.04

Table 2. Specific rates of breakage for various size fractions for thermally treated samples.

Size fractions (mm)	Specific rate of breakage	
	S^{-1}	$min^{-\oplus}$
-1.7+1.18	0.04794	2.88
-1.18+0.6	0.0384	2.30
-0.6+0.3	0.02773	1.66
-0.3+0.15	0.0108	0.65

Table 3. Phase transformations of montmorillonite to other minerals with higher hardness caused by thermal treatment.

	Mineral	Hardness (Mohs)
Before thermal treatment	Montmorillonite	1-2
After thermal treatment	Mullite	6-7
	Cristobalite	6-7
	Cordierite	7-7.5
	Spinel	7.5-8

4.2.2. Effect of particle size

Figure 7 shows the variation in specific rate of breakage versus particle size for the untreated and treated samples. It can be seen that the values increase until 0.6 mm for both conditions (thermal treatment and untreated) and then increase slowly. This means that there is an optimal size fraction (in this condition, approximately 0.6 mm), where the greatest breakage occurs. This can be explained by the fact that a large size fraction is difficult to reduce and ground by the charge medium, thus the grinding efficiency has to be decreased. Variation in the specific rate of breakage values with size fractions were fitted to Eq. 4, and then the specific rate of the breakage parameters A, α, μ, and λ that depend on the properties of the materials and grinding conditions for both conditions (thermal treatment and untreated) are given in Tables 4 and 5.

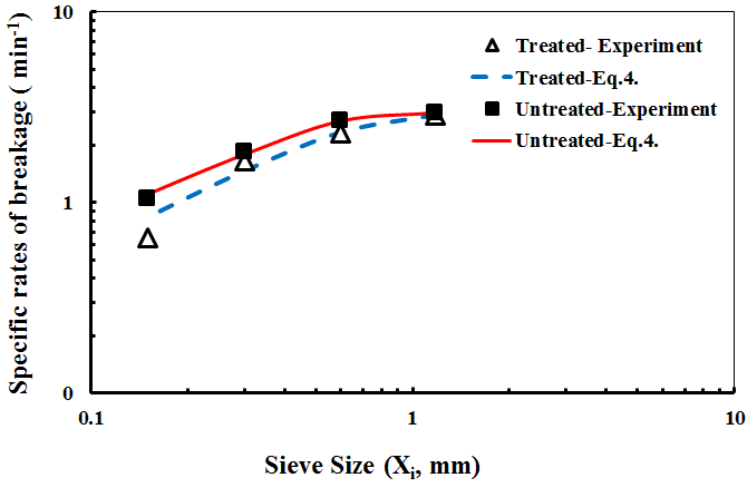

Figure7. Variation in specific rate of breakage with particle size.

Table 4. Results of fitted Eq. 4 relationship for variation in specific rate of breakage with particle size for untreated samples.

Size fractions (mm)	Specific rate of breakage		Error	Squared Error
	Experiment	Model (Eq. 4)		
1.18	2.95	2.9604	0.0104	0.0001
0.6	2.68	2.6837	0.0037	0.0000
0.3	1.85	1.7874	-0.0626	0.0039
0.15	1.04	1.1043	0.0643	0.0041
Sum of squares Errors				0.0082
A (min^{-1})			4.3416	
α			0.7197	
μ (mm)			1.4	
λ			2.5014	

Table 5. Results of fitted Eq. 4 relationship for variation in specific rate of breakage with particle size for thermally treated samples.

Size fractions (mm)	Specific rate of breakage		Error	Squared Error
	Experiment	Model (Eq. 4)		
1.18	2.88	2.8998	0.0098	0.0001
0.6	2.3	2.3430	0.0430	0.0019
0.3	1.66	1.4650	-0.1950	0.0380
0.15	0.65	0.8371	0.1871	0.0350
Sum of squares Errors				0.0750
A (min^{-1})			4.2876	
α			0.8552	
μ (mm)			1.4	
λ			2.0090	

5. Conclusions

The aim of this work was to investigate the effect of thermal treatment on the grinding behavior of manganese ore. SEM analysis showed micro-cracks in the thermally treated manganese sample, and DTA/TG analysis showed that heating at 750 °C led to dehydroxylation of montmorillonite and decomposition of calcite, and that decomposition of montmorillonite to silicate minerals occurred at 850 °C. Montmorillonite mineral with a hardness of 2 was turned to silicate minerals with an average hardness of 7. Dry grinding of size fractions of manganese ore showed that all size fractions of this material followed the first-order kinetics. The specific rate of breakage (Si) values for manganese ore increased with increase in the feed size fractions until 0.6 mm for both conditions (thermal treatment and untreated) and then increased slowly . Therefore, it can be seen that thermal treatment led to decrease in the specific rate of breakage from 1.04 min^{-1} to 0.65 min^{-1} (approximately to 37%) for a size fraction of -0.300+0.15 mm. It, could be expressed that the thermally treated sample was broken slower than the untreated sample in terms of the S_i and "A" values. However, "A" value for the thermally treated sample decreased from 4.36 min^{-1} to 4.28 min^{-1}, which was the maximum S_i value.

Acknowledgments

The authors would like to thank the Iranian Mines and Mining Industries Development and Renovation Organization (IMIDRO) for funding this project, also the Iranian Mineral Processing Research Center (IMPRC) and Imam Khomeini International University (IKIU) for their contribution to this project.

References

[1]. Zhao, R., Han, Y., He, M. and Li, Y. (2017). Grinding kinetics of quartz and chlorite in wet ball milling. Powder Technology. 305: 418-425.

[2]. Somani, A., Nandi, T.K., Pal, S.K. and Majumder, A.K. (2017). Pre-treatment of rocks prior to comminution- A critical review of present practices. International Journal of Mining Science and Technology. 12 (2): 339-348.

[3]. Sheng-Hui, G., Guo, C.H., Jin-Hui, P., Chen, J., Dong-Bo, L. and Li-Jun, L. (2011). Microwave assisted grinding of ilmenite ore. Transactions of Nonferrous Metals Society of China. 21: 2122-2126.

[4]. Chen, G., Xiong, K., Peng, J.H. and Chen, J. (2010). Optimization of combined mechanical activation-roasting parameters of titania slag using response surface methodology. Advanced Powder Technology. 21 (3): 331-335.

[5]. Austin, L.G., Klimpel, R.R. and Luckie, P.T. (1984). Methods for direct experimental determination of the breakage functions, Process engineering of size reduction. Chapter 9. SME-AIME. New York. USA.

[6]. Bozkurt, V. and Ozgur, I. (2007). Dry grinding kinetics of Colemanite. Powder Technology. 176: 88-92.

[7]. Austin, L.G. and Julianelli, K. (2007). Simulation of wet ball milling of iron ore at Carajas, Brazil. International Journal of Mineral Processing. 84: 157-171.

[8]. Omran, M., Fabaitius, T. and Mattila, R. (2015). Thermally assisted liberation of high phosphorus Oolitic iron ore: A comparison between microwave and conventional furnaces. Powder Technology. 269: 7-14.

[9]. Vorster, W., Rowson, N.A. and Kingman, S.W. (2001). The effect of microwave radiation upon the processing of Neves Corvo copper ore. International Journal of Mineral Processing. 63: 29-44.

[10]. Sikong, L. and Bunsin, T. (2009). Mechanical property and cutting rate of microwave treated granite rock. Songklanakarin Journal of Science and Technology. 31 (4): 447-452.

[11]. Zhao, W., Chen, J., Chen, X., Guo, S., Srinivasakannan, C., Chen, G. and Peng, J. (2014). Effect of microwave irradiation on selective heating behavior and magnetic separation characteristics of Panzhihua ilmenite. Applied Surface Science. 300: 171-177.

[12]. Kumar, P., Sahoo, B.K., De, S., Kar, D.D., Chakraborty, S. and Meikap, B.C. (2010). Iron ore grindability improvement by microwave pretreatment. Journal of Industrial and Engineering Chemistry. 16: 805-812.

[13]. Koleini. S.M.J., Barani, K. and Rezaei, B. (2012). The effect of microwave treatment on dry grinding kinetics of Iron ore. Mineral Processing & Extractive Metall. Review. 33:159-169.

[14]. Snow, R. H. (1973). Grinding mill simulation and scale-up of ball mills. Proc. 1st Int. Cof. Particle Technol. IITRI, Chicago.

[15]. Xu, X., Li, X., Liu, F., Wei, W., Wang, X., Liu, K. and Liu, Z. (2017). Batch grinding kinetics of scrap tire rubber particles in a fluidized-bed jet mill. Powder Technology. 305: 389-395.

[16]. Farzanegan, A. and Ghalaei, A.E. (2013). Assessment of grinding flowsheet designs of aghdarreh gold ore processing plant based on circuit simulation approach. 23rd International mining congress & Exhibition of Turkey. pp. 1433-1444.

[17]. Austin, L.G., Klimpel, R.R. and Luckie, P.T. (1984). Process engineering of size reduction. Chapter

9. Methods for Direct Experimental Determination of the Breakage Functions. SME-AIME. New York. USA.

[18]. Austin, L.G. (1972). A review introduction to the mathematical description of grinding as a rate process. Powder Technology. 5: 1-17.

[19]. Yousefi, A.A., Farzanegan, A. and Irannezhad, M. (2001). Breakage function determination software (BFDS). Version 1.0. Amirkabir University of Technology. Faculty of Mining. Metallurgy and Petroleum.

[20]. Faust, G.T. (1950). Thermal analysis studies on carbonates. I. Aragonite and calcite. American Mineralogist. 35 (3-4): 207-224.

[21]. Keskinkilic, E., Pournaderi, S., Geveci, A. and Topkaya, Y.A. (2012). Calcination characteristics of laterite ores from the central region of Anatolia. The Journal of the Southern African Institute of Mining and Metallurgy. 112: 877-882.

[22]. Cuthbert, F.L. and Rowland, R.A. (1947). Differential thermal analysis of some carbonate minerals. American Mineralogist. 32 (3-4): 111-116.

[23]. Foldvari, M. (2011). Handbook of Thermogravimetric System of Minerals and Its Use in Geological Practice. Occasional Papers of the Geological Institute of Hungury. Vol. 213.

[24]. Mozas, T., Bruque, S. and Rodriguez, A. (1980). Effect of thermal treatment on lanthanide montmorillonite: dehydration. Clay Minerals. 15: 421-428.

[25]. Fernandez, M., Alba, M.D. and Torres Sanchez, R.M. (2013). Effect of thermal and mechanical treatments on montmorillonite homoionized with mono- and polyvalent cation: Insight into the surface and structural changes. Colloids and Surfaces A: Physicochemical and Engineering Aspects. 423: 1-10.

اثر عملیات حرارتی بر ثابت نرخ شکست کانسنگ منگنز

منیره حشامی و رحمان احمدی*

گروه مهندسی معدن، دانشکده فنی و مهندسی، دانشگاه بین‌المللی امام خمینی (ره)، ایران

ارسال ۲۰۱۷/۸/۲۲، پذیرش ۲۰۱۷/۱۰/۲۶

* نویسنده مسئول مکاتبات: ra.ahmadi@eng.ikiu.ac.ir

چکیده:

هدف این مطالعه بررسی اثر عملیات حرارتی بر رفتار خردایش کانسنگ منگنز، در محدوده‌های ابعادی مختلف ۱/۱۸+ ۱/۷-، ۰/۶+ ۱/۱۸-، ۰/۳+ ۰/۶- و ۰/۱۵+ ۰/۳- میلی‌متر است. برای مطالعات تابع انتخاب از نرم‌افزار تعیین تابع شکست (BFDS) استفاده شد. نتایج آنالیز SEM نشان داد، حرارت باعث ایجاد میکرو ترک‌ها در نمونه منگنز شده است. بر اساس نتایج به دست آمده از آنالیز حرارتی (DTA/TG)، حرارت تا دمای ۷۵۰°C منجر به دی هیدروکسیلیشن کانی‌های رسی و همچنین تجزیه کلسیت و در دمای ۸۵۰°C منجر به تجزیه کانی رسی مونت‌موریلونیت به کانی‌های سیلیکاته شده است. کانی مونت‌موریلونیت با سختی ۲ بر اثر حرارت به کانی‌های سیلیکاته با سختی به طور میانگین ۷ تبدیل شده است. نتایج تابع انتخاب نشان می‌دهد که عملیات حرارتی منجر به کاهش ثابت نرخ شکست برای محدوده ابعادی ۰/۱۵ mm+ ۰/۳- از $1/04\ min^{-1}$ تا $0/65\ min^{-1}$ (تقریباً ۳۷٪) شده است که بیانگر این است، نمونه تحت عملیات حرارتی نسبت به نمونه بدون عملیات حرارتی به آرامی شکسته شده است. همچنین پارامتر A که بیشینه ثابت نرخ شکست است، برای نمونه تحت حرارت از $4/36\ min^{-1}$ تا $4/28\ min^{-1}$ کاهش یافته است. علاوه بر این، نتایج تابع انتخاب نشان داد که همه‌ی محدوده‌های ابعادی از سینتیک مرتبه اول تبعیت می‌کند.

کلمات کلیدی: عملیات حرارتی، ثابت نرخ شکست، سینتیک خردایش، نرم‌افزار تعیین تابع شکست، کانسنگ منگنز.